siRNA targeting of PRDX3 enhances cisplatin-induced apoptosis in ovarian cancer cells through the suppression of the NF-κB signaling pathway

JIE DUAN[1], YAN LANG[1], CHENGWEN SONG[2], JUN XIONG[1], YAN WANG[1] and YANG YAN[1]

[1]Gynecology, Maternal and Child Health Hospital of Hubei Province;
[2]Wuhan General Hospital of Guangzhou Military, Wuhan, Hubei 430070, P.R. China

Abstract. The overexpression of peroxiredoxins (prxs) has been shown to be associated with the development, progression and drug resistance of cancer. However, the role of the prxs in the drug resistance of ovarian cancer is unknown. The present study aimed to investigate the effect and mechanism of the downregulation of PRDX3 on cisplatin-induced ovarian cancer cell apoptosis. The expression of PRDX3 in ovarian cancer was examined by immunohistochemistry. The effect on cisplatin-induced ovarian cancer apoptosis by the silencing of PRDX3 was determined by cell proliferation and colony formation assays and the examination of tumor growth in the nude mice. To further investigate the mechanism behind the downregulation of PRDX3, the expression of the anti-apoptotic proteins Bcl-2 and Bcl-XL and the pro-apoptotic proteins Bax, Caspase-3 and Caspase-9 was examined in various ovarian cancer cells. The results showed that the aberrant expression of PRDX3 in ovarian cancer may be a factor responsible for its progression. SKOV3 ovarian cancer cells transfected with PRDX3/small interfering (Si)-1 efficiently downregulated the expression of PRDX3 and thus decreased the growth of the SKOV3 cells *in vitro* and *in vivo*. Furthermore, the silencing of PRDX3 triggered cisplatin-mediated apoptosis in the ovarian cancer cells, which may act through suppression of the NF-κB signaling pathway. These data suggest a new mechanism by which the downregulation of PRDX3 enhances cisplatin-induced ovarian cancer cell apoptosis. This mechanism may provide new evidence for the potential application of PRDX3-siRNA in ovarian cancer therapy.

Introduction

Ovarian cancer continues to be the most frequent cause of cancer mortality among females in Western Europe and the United States, with the highest mortality rate of all gynecological malignancies (1). The most common histological subtype of ovarian cancer is epithelioid cancer (serous, endometrioid, mucinous and clear cell), accounting for 90% of ovarian malignancies (2,3). Although >70% of patients have increased 5-year survival rates subsequent to surgery followed by chemotherapy plus second-line therapies, a number of tumor types fail to respond to chemotherapy. This is due to the fact that in consecutive chemotherapy, these tumors appear to become less sensitive or resistant to chemotherapeutic drugs. The intolerable side-effects of the systemic treatment with chemotherapy means that the development of novel and effective therapeutic modalities and the identification of new rational targets for these novel therapies are required (4).

Organisms living under aerobic conditions are exposed to reactive oxygen species (ROS), including superoxide anions (O_2^-), hydrogen peroxide (H_2O_2) and nitric oxide (NO), which are generated by the redox metabolism mainly in the mitochondria (5). A number of studies have demonstrated that ROS in small amounts participate in numerous physiological processes, including cell proliferation, differentiation and apoptosis and the modulation of transcription factors and signal transduction pathways (6,7). Cancer cells have been demonstrated to possess higher levels of intracellular ROS due to increased cellular respiration and are believed to have the potential to oxidize macromolecules, induce DNA mutation, impair protein function and peroxidize lipids, thus leading to the development of tumors (8,9). However, to facilitate the development of tumors, numerous antioxidative systems have been developed to maintain an appropriate level of ROS, which include antioxidant enzymes such as glutathione peroxidases (GPXs), superoxide dismutases (SODs), catalases and the recently identified rapidly growing family of peroxiredoxins (Prxs) (10,11).

Prxs have been shown to be involved in diverse cellular roles, including the control of cell proliferation, differentiation and apoptosis, the protection of oxidant-sensitive proteins, the regulation of cellular H_2O_2 and redox regulation (12,13). Recent studies have suggested that Prxs are involved in the development, progression and drug resistance of cancers (14,15). As a member of the Prx family, PRDX3 is overexpressed in a number of diverse tumors, including hepatocellular carcinoma and lung and prostate cancer (16-18).

Correspondence to: Dr Jie Duan, Gynecology, Maternal and Child Health Hospital of Hubei Province, No. 745 Wuluo Road, Wuchang District, Wuhan, Hubei 430070, P.R. China
E-mail: william1998_0402@163.com

To the best of our knowledge, there has only been one study describing the potential role of PRDX3 in ovarian cancer, in which PRDX3 was determined to be responsible for resistance to platinum-based chemotherapies (19). As an anti-apoptotic protein for tumor cell proliferation and survival, therapeutic strategies targeting PRDX3 may therefore be effective broad-spectrum anticancer agents.

In the present study, the focus was on the role and mechanism behind the downregulation of PRDX3 in cisplatin-induced ovarian cancer cell apoptosis. For the first time we reported that the overexpression of PRDX3 was observed in ovarian cancer and that the PRDX3 knockdown resulted in accelerated cisplatin-induced cell apoptosis through suppression of the NF-κB signaling pathway. This may provide a new insight into anticancer therapy for ovarian cancer.

Materials and methods

Tissue samples. In total, 104 paraffin-embedded ovarian cancer tissues and paired non-cancerous tissues were surgically obtained from the Maternal and Child Health Hospital of Hubei Province, Wuhan, Hubei, China, between 2005 and 2011. All the procedures were approved by the research ethics committee of the Maternal and Child Health Hospital of Hubei Province. All the patients agreed to the procedure and signed consent forms. None of the patients had received chemotherapy or radiation therapy prior to the surgery. The staging and grading were performed by two experienced gynecological pathologists according to the criteria of the International Federation of Gynaecologists and Obstetricians (FIGO) and the World Health Organization (WHO). The median patient age was 56 years (range, 33-72 years). Detailed patient characteristics are presented in Table I.

Immunohistochemistry and staining score evaluation. The paraffin slices were successively incubated for 5 min in a series of xylene and ethanol baths of decreasing concentration. The antigen was retrieved by boiling the slices in a 0.1 M Na citrate buffer (pH 6.0). The endogenous peroxidase was inhibited by 3% H_2O_2. The monoclonal mouse anti-PRDX3 antibodies (Abcam, Cambridge, UK), diluted 100-fold in 1% BSA, were applied and incubated overnight at 4˚C. The incubation with the horseradish peroxidase (HRP)-conjugated goat anti-mouse antibodies at 37˚C for 30 min was followed by the reaction with the 3,3'-diaminobenzidine substrate solution and counterstaining with Mayer's hematoxylin. All the steps were performed in a moist chamber.

The expression of PRDX3 was scored based on the intensity of the staining and the percentage of positively stained cells. Staining intensity was scored as follows: lack of staining, 0, weak staining 1, moderate staining, 2 and strong staining, 3. The percentage of the positively stained cells was scored as 0 if no staining was observed or if it was present in <5% of the cells; 1 if positive staining was present in 5-25% of the cells; 2 if positive staining was present in 25-50% of the cells; 3 if positive staining was present in 50-75% of the cells; and 4 if positive staining was present in in >75% of cells. The score for each section was measured as the staining intensity x the percentage of the positively stained cells. The result was defined as negative (-, score of 0), weakly positive (+, score of

1-3), moderately positive (++, score of 4-7) or strongly positive (+++, score of 8-12). The slides were examined separately by two independent pathologists who had no prior knowledge of each patient's clinical information. Any discrepancies between the two evaluators were resolved by a re-evaluation and careful discussion until agreement was reached.

RNA interference experiments. First, the expression of PRDX3 was examined in the HO-8910, SKOV3, OVCAR-3 ovarian cancer cell lines (ATCC, Manassas, VA, USA). To knock down the PRDX3 expression, a pGCsi-U6/Neo/GFP vector was used that encoded a small hairpin RNA directed against the target gene in the SKOV3 ovarian cancer cells. The target sequences for PRDX3 were 5'-ACCTTCTGAAAGTACTCTT-3' [small interfering (si)RNA-1], 5'-CTTTAGACGAATCAATTCA-3' (siRNA-2) and 5'-CGTACGACCCACTGTCGTC-3' (siRNA-3). As a negative control, the shRNA vector without hairpin oligonucleotides (siRNA-mock) was used. For the transfection, the ovarian cancer cells were seeded to achieve 70-80% confluence and then transfected in serum-free medium for 6 h with Lipofectamine 2000 (Invitrogen, Carlsbad, CA, USA) and siRNA-PRDX3 or the siRNA-mock. Subsequent to 48 h, the cells were harvested and a limited dilution was performed in 96-well plates for the generation of individual cell clones. Three weeks later, the levels of PRDX3 expression in the cell clones that had been transfected with siRNA-PRDX3 or the siRNA-mock, were characterized by a western blot analysis for the PRDX3 protein.

Western blot analysis. The cells were lysed in a lysis buffer (62.5 mM Tris-HCl, pH 6.8, 2% SDS, 10% glycerol, 50 mM dithiothreitol and 0.01% bromophenol blue). The cell extract protein amounts were quantified using the Bicinchoninic Acid (BCA) Protein Assay kit (Beyotime, Shanghai, China). Equivalent amounts of protein (50 µg) were separated using 12% sodium dodecyl sulfate-polyacrylamide gel electrophoresis (SDS-PAGE) and then transferred to a polyvinylidene fluoride (PVDF) membrane (Millipore Corporation, Billerica, MA, USA). The blots were probed with specific antibodies for PRDX3 (1:1000, ab16751; Abcam), p-NF-κB (1:1000, sc135769; Santa Cruz Biotechnology Inc., Santa Cruz, CA, USA), Bcl-2 (1:500, ab692, Abcam), Bcl-XL (1:1000, sc8392; Santa Cruz Biotechnology Inc.), Bax (1:1000, ab5714; Abcam), caspase-3 (1:3000, ab32351, Abcam), caspase-9 (1:1000, sc81650; Santa Cruz Biotechnology Inc.) and β-actin (1:1000, ab3280; Abcam) followed by a secondary detection step with goat anti-mouse IgG (Abcam). The immunoreactive proteins were revealed by an Enhanced Chemiluminescence (ECL) kit (Pierce, Rockford, IL, USA).

Cell proliferation assay. A cell proliferation assay was performed using the Cell-Counting kit (CCK)-8 (Dojindo, Kumamoto, Japan) to analyze the proliferation potential of the parental cells, empty vector and siRNA-PRDX3-transfected cells treated with/without cisplatin. The cells were harvested and plated in 96-well plates at $1x10^3$ cells/well and maintained at 37˚C in a humidified incubator. At the indicated time-points, 10 µl of the CCK-8 solution were added and incubated for 1.5 h and the number of viable cells in each well was calculated by measuring the absorbance at a wavelength of 450 nm.

Colony formation assay. The colony formation assay was performed to measure the cell growth according to the protocol described previously (20), with certain modifications. Identical numbers of parental cells, empty vector and siRNA-PRDX3-transfected cells treated with/without cisplatin were seeded in 6-well tissue-culture plates to form colonies. Subsequent to incubation for 10 days, the number of colonies (≥20 cells) within a field was counted under a light microscope at a magnification of x200. For each test, a total of five fields were selected at random and the numbers were averaged. For the calculation of the colony forming ability, the following formula was used: colony forming efficiency = number of colonies / number of inoculated cells x 100.

Tumorigenicity assays in athymic mice. Male, 6-8-week old, BALB/c nude (nu/nu) mice were purchased from Slac Laboratory Animal Co., Ltd. (Shanghai, China) and used for the *in vivo* studies. The mice were randomly divided into six groups (n=8) and injected with the following: i) $5x10^6$ SKOV3 cells in 100 μl PBS; ii) $5x10^6$ SKOV3/Si-Mock cells in 100 μl PBS; iii) $5x10^6$ SKOV3/Si-1 cells in 100 μl PBS; iv) $5x10^6$ SKOV3 cells plus 0.1 mg cisplatin in 100 μl PBS; v) $5x10^6$ SKOV3/Si-Mock cells plus 0.1 mg cisplatin in 100 μl PBS; and vi) $5x10^6$ SKOV3/Si-1 cells plus 0.1 mg cisplatin in 100 μl PBS (5 mg/kg body weight). The $5x10^6$ cells were subcutaneously injected into the left back flank of these animals. Cisplatin was administered by the intraperitoneal route on day 6 subsequent to the implantation of the tumor cells and again when the tumor diameter reached ~5 mm (every week, 4 times). The tumor variables were measured every three days by an electronic caliper and the tumor volume was calculated using the formula: tumor volume (mm^3) = 0.52 x length (mm) x width^2 (mm^2). The measurements began in the first week when the tumor mass was well-established. A third operator evaluated the morphometric variables in a coded and blinded maner. The tissue samples were harvested for terminal deoxynucleotidyl transferase-mediated dUTP nick end-labeling (TUNEL) analysis.

TUNEL assay. TUNEL analysis was performed with an *in situ* Cell Death Detection kit (Roche, Basel, Switzerland). The cell apoptosis index was quantified by determining the percentage of the positively stained cells for all of the nuclei in 20 randomly chosen fields at a magnification of x200. Slides of the apoptosis studies were quantified in a blind manner by two independent reviewers at two differing times.

Statistical analysis. Data are presented as the mean ± standard deviation. Statistical analyses were performed by SPSS 13.0 software. Differences among the groups were determined by an ANOVA analysis and the comparison between two groups was analyzed by the Student's t-test. Nominal variables were compared using a cross-tabulation test. $P<0.05$ was considered to indicate a statistically significant difference.

Results

Association between PRDX3 expression and the clinicopathological characteristics of ovarian cancer. To investigate the role of PRDX3 in the progression of ovarian cancer, immunohistochemistry was used to assess the PRDX3 expression levels in the paraffin-embedded tissues. The association between PRDX3 expression and the clinicopathological characteristics of the ovarian cancer tissues is shown in Table I. PRDX3 was heavily stained in the cytoplasm and nuclei of the cancer tissues (12.5% +, 47.1% ++ and 32.7% +++), but little staining was observed in the adjacent non-cancerous tissues (35.5% - and 64.5% +). The difference between the cancerous and non-cancerous tissues was significant ($P<0.05$). The patients with serous ovarian cancer accounted for 58.7% of the total cases. Serous ovarian cancer mostly presented at FIGO stage III or IV (FIGO I + II, 32.8% and FIGO III + IV, 67.2%) and a significant difference was observed between stages I + II and III + IV ($P<0.05$) in the various types of ovarian cancer. With regard to tumor differentiation, significant differences were identified in the PRDX3 expression among the well-differentiated, moderately-differentiated and poorly-differentiated serous ovarian cancer samples ($P<0.05$). With respect to the mucinous, endometrioid and clear cell types, there were significant differences between stages I + II and III + IV in the endometrioid ovarian cancer samples, but not in the mucinous or clear cell types. With regard to the tumor differentiation of the mucinous, endometrioid and clear cell carcinomas, the differences in the PRDX3 expression among the well-, moderately- and poorly-differentiated carcinomas were not significant. Only slight differences in the PRDX3 expression were observed with respect to the histological subtype, age at first diagnosis and lymph node metastasis ($P>0.05$).

Inhibition of PRDX3 expression in the ovarian cancer cells. To select the optimal cells to be transfected, the expression of PRDX3 was detected in three cell lines (HO-8910, SKOV3 and OVCAR-3) , as shown in Fig. 1A. The expression level of PRDX3 in the HO-8910, SKOV3 and OVCAR-3 cell lines showed no significant difference, with the lowest expression observed in the HO-8910 cells and the highest in the SKOV3 cells. To investigate the biological significance of PRDX3 on the ovarian cancer cells, three siRNA expression vectors (Si-1, Si-2 and Si-3) specific to the PRDX3 transcripts were constructed and transfected into the ovarian cancer SKOV3 cells that endogenously expressed a high level of PRDX3 (Fig. 1A). A knockdown effect was observed by western blot analysis and SKOV3/Si-1 was observed to be the most effective when compared with the SKOV3/Si-Mock (Fig. 1B). The successful establishment of the PRDX3 gene silent ovarian cancer cell clone provided a useful tool for the investigation into the function of PRDX3 in the growth of the ovarian cancer cells.

Effect of PRDX3-siRNA on the growth of the ovarian cancer cells. To examine the effect of PRDX3 on the growth of the ovarian cancer cells, the dynamics of SKOV3, SKOV3/Si-Mock and SKOV3/Si-1 cell growth were determined by a cell proliferation assay. Following a 7-day period, the growth of the SKOV3/Si-1 cells was much slower compared with the SKOV3 or SKOV3/Si-Mock groups (Fig. 2A). The other pattern of inhibition for the PRDX3 expression in the ovarian cancer cells was achieved in the colony formation assay. Consequently, the average colony number of the SKOV3/Si-1 cells was decreased compared with the SKOV3 or SKOV3/Si-Mock groups. This difference was significant ($P<0.05$; Fig. 2B). To further explore the reason behind the decrease in cell viability, the tumori-

Table I. Associations between the expression of PRDX3 and the clinicopathological parameters in ovarian cancer.

Parameters	Cases (n)	PRDX3 expression				P-value
		-	+	++	+++	
Age at first diagnosis						
<56 years	45	2	5	22	16	0.691
≥56 years	59	6	8	27	18	
Serous						
I/II	20	3	4	9	4	0.045[a]
III/IV	41	1	2	22	16	
Well-differentiated	21	2	2	15	2	0.028[b]
Moderately-differentiated	23	2	3	11	7	
Poorly-differentiated	17	0	1	5	11	
Mucinous						
I/II	8	1	2	3	2	0.173[a]
III/IV	11	1	1	9	0	
Well-differentiated	9	2	2	3	2	0.251[b]
Moderately-differentiated	6	0	1	5	0	
Poorly-differentiated	4	0	0	4	0	
Endometrioid						
I/II	4	1	2	1	0	0.032[a]
III/IV	7	0	0	1	6	
Well-differentiated	4	1	2	0	1	0.278[b]
Moderately-differentiated	4	0	0	1	3	
Poorly-differentiated	3	0	0	1	2	
Clear cell						
I/II	4	1	1	2	0	0.114[a]
III/IV	9	0	1	2	6	
Well-differentiated	5	0	1	2	2	0.71[b]
Moderately-differentiated	3	0	1	1	1	
Poorly-differentiated	5	1	0	1	3	
Lymph node metastasis						
Negative	82	6	8	39	29	0.352
Positive	22	2	5	10	5	

[a]Statistical difference between FIGO stages I/II and III/IV; [b]statistical difference among the well-, moderately- and poorly-differentiated cancer types. -, negative; +, weakly positive; ++, moderately positive; +++, strongly positive; FIGO, International Federation of Gynaecologists and Obstetricians.
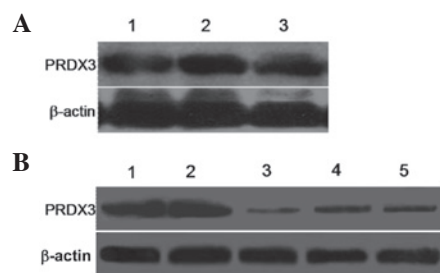

Figure 1. Expression of PRDX3 analyzed by western blot assay. (A) Expression of PRDX3 in three ovarian cancer cell lines (HO-8910, SKOV3 and OVCAR-3) was detected. β-actin served as an internal control. Lanes 1, HO-8910 cells; 2, SKOV3 cells; 3, OVCAR-3 cells. (B) Western blot analysis of PRDX3 in SKOV3 cells transfected with control (Si-Mock) or small interfering RNA (Si-1, Si-2 and Si-3). β-actin served as an internal control. Lanes 1, SKOV3 cells; 2, SKOV3/Si-Mock; 3, SKOV3/Si-1; 4, SKOV3/Si-2; 5, SKOV3/Si-3.

genicity of the SKOV3/Si-1 cells was examined, as shown in Fig. 2C. The tumor size in the nude mice injected with the SKOV3/Si-1 cells was significantly smaller than that in the mice injected with the SKOV3/Si-Mock cells ($P<0.05$). This was associated with the enhanced induction of apoptosis, as shown by Fig. 4A.

PRDX3-siRNA enhances cisplatin-induced ovarian cancer cell apoptosis. To investigate the impact of the PRDX3-siRNA on cisplatin-induced ovarian cancer cell apoptosis, the effect of cisplatin on the growth of the SKOV3 cells was firstly examined by a cell proliferation assay. The SKOV3 cells were treated with 0, 1, 2, 3 and 4 μg/ml cisplatin for 1, 2, 3, 4 and 5 days, respectively (Fig. 3). The addition of cisplatin to the

culture media inhibited the proliferation of the SKOV3 cells in a dose-dependent manner. When the cisplatin concentration was 3 μg/ml, the effect was more evident.

To study whether the PRDX3-siRNA was able to enhance cisplatin-induced ovarian cancer cell apoptosis, the SKOV3/Si-1 and SKOV3/Si-Mock cells were treated with or without 3 μg/ml cisplatin. The cells were then collected and analyzed by cell proliferation (Fig. 3B) and colony formation assays (Fig. 3C). These assays revealed a marked reduction in the cisplatin-treated SKOV3/Si-1 cells compared with the cisplatin-treated SKOV3/Si-Mock cells for which no knockdown effect was observed. The tumor size of the nude mice injected with the cisplatin-treated SKOV3/Si-1 cells was significantly smaller than that of the mice injected with the cisplatin-treated SKOV3/Si-Mock cells (Fig. 3D). This was associated with the enhanced induction of apoptosis, as shown by Fig. 4A.

Cisplatin-induced apoptosis may be enhanced by PRDX3-siRNA via the activation of the caspase, apoptosis- related proteins. The NF-κB-mediated expression of Bcl-2 and Bcl-XL is known to protect cancer cells from apoptosis, whereas Bax, caspase-3 and caspase-9 inhibit cancer cell growth and induce apoptosis. To validate whether PRDX3-siRNA was able to enhance cisplatin-induced apoptosis in the ovarian cancer cells via the activation of the caspase and apoptosis-related proteins, the expression of these proteins was investigated. The pro-apoptosis proteins Bax, caspase-3 and caspase-9 were analyzed in the SKOV3/Si-1 and SKOV3/Si-Mock cells treated with or without cisplatin (3 μg/ml). The caspase-3 protein was activated and the Bax expression was increased in the SKOV3/Si-1 or SKOV3/Si-1 cells treated with cisplatin, but not in the SKOV3/Si-Mock cells treated with or without cisplatin. Additionally, the activation of the caspase-9 protein was observed in the SKOV3/Si-1 or SKOV3/Si-1 cells treated with
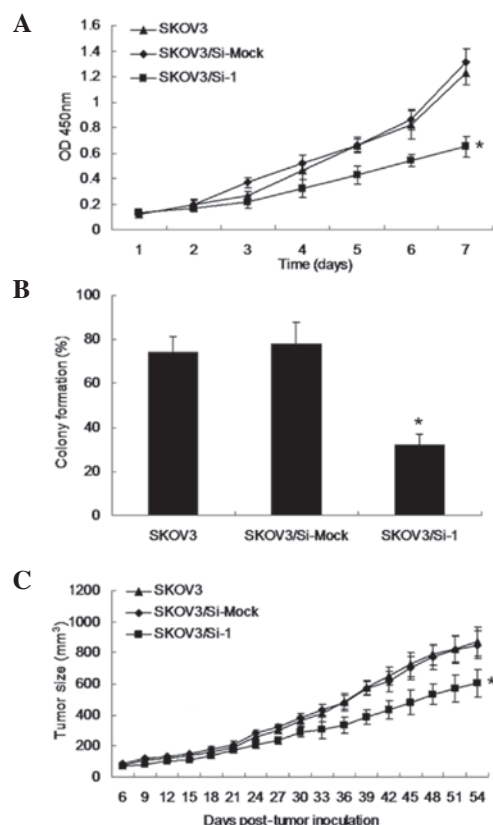
Figure 2. Effect of PRDX3-small interfering (si)RNA on the growth of the SKOV3 ovarian cancer cells. (A) The growth of the SKOV3, SKOV3/Si-Mock and SKOV3/Si-1 cells was determined by CCK-8 assay. (B) The growth of the SKOV3, SKOV3/Si-Mock and SKOV3/Si-1 cells was examined by a colony formation assay. * vs. the SKOV3/Si-Mock or SKOV3 group, P<0.05. (C) Graphical representation of the tumor size over time in mice injected with SKOV3, SKOV3/Si-Mock and SKOV3/Si-1 cells. Data are expressed as the mean ± SEM of three independent experiments. CCK-8, Cell-Counting kit; si, small interfering.
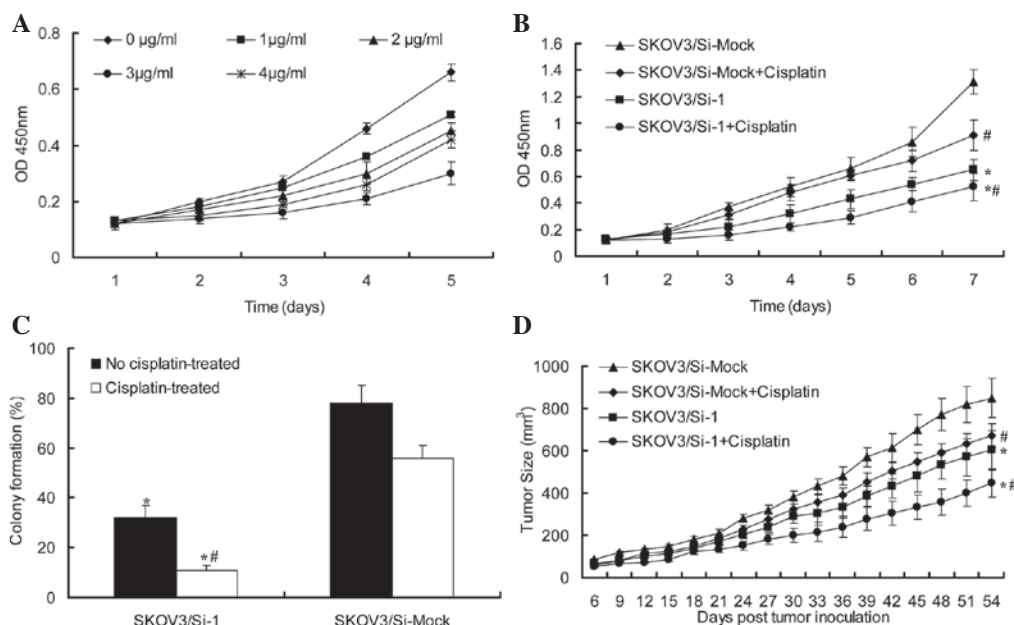
Figure 3. PRDX3-siRNA enhanced cisplatin-induced ovarian cancer cell apoptosis. (A) Effect of cisplatin on SKOV3 ovarian cancer cells. Under the stimulation of various concentration of cisplatin (0, 1, 2, 3 and 4 μg/ml) for 1, 2, 3, 4 and 5 days, respectively, the absorbance of SKOV3 cells was observed by CCK-8 assay. (B) Growth of SKOV3/Si-Mock and SKOV3/Si-1 cells with/without treatment of 3 μg/ml cisplatin was examined by CCK-8 assay. (C) Growth of SKOV3/Si-Mock and SKOV3/Si-1 cells with/without treatment of 3 μg/ml cisplatin was examined by colony formation assay. * vs. SKOV3/Si-Mock group, P<0.05, # vs. No cisplatin-treated group, P<0.05. (D) Graphical representation of the tumor size over time in mice injected with SKOV3/Si-Mock or SKOV3/Si-1 cells with/without treatment of 3 μg/ml cisplatin (n=8). CCK-8, Cell-Counting kit; si, small interfering.
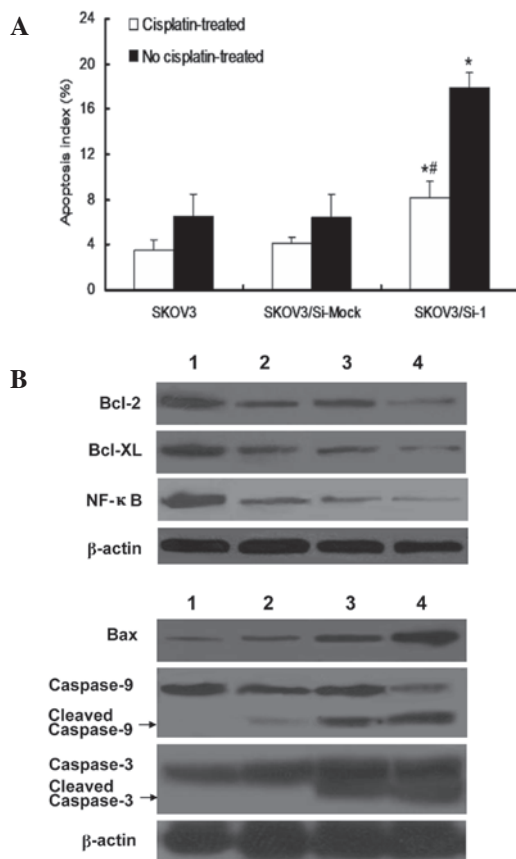
Figure 4. PRDX3-siRNA enhances cisplatin-induced ovarian cancer cell apoptosis via the NF-κB signaling pathway. (A) Apoptotic index of the various ovarian cancer tissues. In the tumorigenicity assay, tumor tissue samples were collected for the TUNEL analysis. The apoptotic index of the groups was counted and calculated as a ratio of the apoptotic cell number to the total cell number in each field. * vs. SKOV3/Si-Mock or SKOV3 groups, P<0.05 and # vs. No cisplatin-treated group, P<0.05. (B) Western blot analysis of the expression of apoptosis-related proteins Bcl-2, Bcl-XL, NF-κB p65, Bax, Caspase-3 and Caspase-9 in the SKOV3/Si-Mock or SKOV3/Si-1 cells with/without treatment of cisplatin. Lanes 1, SKOV3/Si-Mock; 2, SKOV3/Si-Mock+Cisplatin; 3, SKOV3/Si-1; 4, SKOV3/Si-1+Cisplatin; TUNEL, terminal deoxynucleotidyl transferase-mediated dUTP nick end-labeling; si, small interfering.

cisplatin and the partial activation of caspase-9 was observed in the cisplatin-treated SKOV/Si-Mock cells, but not in the SKOV3/Si-Mock cells.

Elevated levels of the anti-apoptotic proteins Bcl-2 and Bcl-XL confer chemoresistance, therefore the participation of Bcl-2 and Bcl-XL was examined by a western blot analysis. As shown in Fig. 4B, the PRDX3-siRNA was able to markedly downregulate the expression of the Bcl-2 and Bcl-XL proteins in the cisplatin-treated SKOV3/Si-1 cells compared with the SKOV3/Si-Mock cells treated with/without cisplatin. The phosphorylation of NF-κB p65 was examined and the results showed a significant inhibition in the cisplatin-treated SKOV3/Si-1 cells.

Discussion

Ovarian cancer remains a leading gynecological malignancy across the world. As it possesses the highest mortality rate among the gynecological cancers, ovarian cancer has become the most lethal malignancy of the female reproductive system (2).

To extend the long-term survival rate, certain improvements have been made, including the modulation of cellular chemosensitivity, the reversal of tumor resistance and the increase in the therapeutic effects of chemotherapy. However, due to the dose-dependent toxicity, eventual tumor recurrence and emergence of drug-resistance in the disease, the therapeutic efficacy remains poor (21). Mounting evidence suggests that cancer cells exhibit increased intrinsic ROS. In order to protect themselves against oxidative stress induced by the ROS, cells use several antioxidants or reductants to maintain the intracellular redox environment in a highly reduced state. The upregulation of antioxidant enzymes, particularly in the mitochondria, would provide cancer cells with certain survival advantages under intrinsically high oxidative conditions (22). As a significant cellular antioxidant, PRDX3 may regulate the physiological levels of H_2O_2, thus protecting cells against the apoptosis caused by high levels of H_2O_2. Increased mitochondrial ROS generation and the disturbance of prx production in cancer cells may lead to oxidative stress and hypoxic microenvironments, subsequently leading to the induction of apoptosis (17). Increased expression levels of PRDX3 were therefore assumed to protect tumor cells against the hypoxia microenvironment and drug-induced H_2O_2-dependent apoptosis.

To the best of our knowledge, several studies have shown that the PRDX3 protein is overexpressed in numerous types of cancer, including lung, breast and prostate cancer and hepatocellular carcinoma (16-18), but few studies have reported the correlation between the overexpression of PRDX3 and the progress of ovarian cancer. The present study examined the association between the expression of PRDX3 and the clinicopathological parameters in various types of ovarian cancers. The results showed that the high expression of PRDX3 in serous ovarian cancer was associated with poorly-differentiated cancer cells. Moreover, FIGO stage IV/metastatic serous ovarian cancer samples were shown to overexpress PRDX3 at the highest level, which suggested that the PRDX3 expression was significantly associated with increasing cancer progression. A similar tendency was evident in the mucinous, endometrioid and clear cell types of ovarian cancer, but the differences between stages I + II and III + IV, among well-, moderately- and poorly-differentiated ovarian cancer were not significant. This result should be further verified due to the limited number of cases. The most common type of ovarian cancer is serous, therefore, inhibiting the mitochondrial antioxidant enzyme PRDX3 in the ovarian cancer cells may act as an effective cancer therapeutic method.

Cisplatin has been shown to induce apoptosis in various types of cancer cells. Despite the great efficacy at treating these certain types of cancer, the side-effects or resistance to cisplatin undermine its curative potential (23). Based on the the previously stated factors, we assumed that downregulation of the PRDX3 protein would enhance cisplatin-induced ovarian cancer cell apoptosis. Therefore, ovarian cancer cells stably transfected with PRDX3-siRNA were first established by the RNAi approach, in which the target gene was efficiently knocked down. In the present study, the SKOV3 and OVCAR-3 cell lines were stably transfected with PRDX3-siRNA simultaneously, but the transfection efficiency of OVCAR-3 was not high. This may have been affected by the dose or toxicity of the transfection reagent or by the transfection time. The gene-silenced clones

of the SKOV3 cells transfected with the PRDX3-siRNA were screened by a limited dilution method and verified by western blot analysis (Fig. 1B). Functional analysis using the siRNA of PRDX3 strongly supported the involvement of PRDX3 in the development and progression of ovarian cancer. As shown in Fig. 2, the proliferation rate of the SKOV3 cells following PRDX3 knockdown was reduced significantly, whereas the proliferation of the SKOV3/Si-Mock cells was not inhibited. To further explore whether the silencing of PRDX3 reversed the resistance of the ovarian cancer cells to cisplatin, a series of experiments were designed. The results showed that when comparing the proliferative activity of the SKOV3/Si-Mock cells treated with cisplatin and the SKOV3/Si-1 cells, the proliferation of the SKOV3/Si-1 cells treated with cisplatin significantly decreased ($P<0.05$). The enhanced antitumor efficacy *in vivo* was associated with the enhanced induction of apoptosis, as verified by the TUNEL analysis (Fig. 4). All the data suggested that the combination of the PRDX3-siRNA and cisplatin showed a synergistic anti-cancer effect.

PRDX3 is one of the most significant antioxidant enzymes that modulates intracellular signaling pathways correlated to apoptosis and cell proliferation. Understanding the anticancer mechanism of PRDX3, with the goal of enhancing its efficacy as a valuable adjunct or single agent in anticancer therapy, is extremely important. NF-κB has been implicated in carcinogenesis and the development of drug resistance in cancer cells (24). A previous study indicated that NF-κB was the most reliable target of the combination chemotherapeutic treatment to overcome drug resistance (25). It is well-known that the NF-κB-mediated expression of Bcl-2 and Bcl-XL protects cancer cells from apoptosis, whereas Bax, caspase-3, and caspase-9 inhibit cancer cell growth and induce apoptosis. Therefore, whether PRDX3-siRNA in combination with cisplatin is able to disrupt the NF-κB pathway or not is extremely significant. The present study showed that a significant inhibition of the phosphorylation of NF-κB p65 and a decrease in the levels of the anti-apoptotic proteins, Bcl-2 and Bcl-XL, were induced in the cisplatin-treated SKOV3/Si-1 cells. By contrast, an increase in the level of Bax and the activation of caspase-3 and caspase-9 were observed in the cisplatin-treated SKOV3/Si-1 cells.

In conclusion, these results suggest that silencing the expression of PRDX3 may enhance cisplatin-induced ovarian cancer cell apoptosis through the suppression of the NF-κB signaling pathway. This provides new evidence for the potential application of PRDX3-siRNA as a chemosensitizer in ovarian cancer therapy.

Acknowledgements

References

1. Wolf JK and Jenkins AD: Gene therapy for ovarian cancer (Review). Int J Oncol 21: 461-468, 2002.
2. Felix AS, Stone RA, Bowser R, Chivukula M, Edwards RP, Weissfeld JL and Linkov F: Comparison of survival outcomes between patients with malignant mixed mullerian tumors and high-grade endometrioid, clear cell, and papillary serous endometrial cancers. Int J Gynecol Cancer 21: 877-884, 2011.
3. Lalwani N, Prasad SR, Vikram R, Shanbhogue AK, Huettner PC and Fasih N: Histologic, molecular, and cytogenetic features of ovarian cancers: implications for diagnosis and treatment. Radiographics 31: 625-646, 2011.
4. Ledermann J, Harter P, Gourley C, et al: Olaparib maintenance therapy in platinum-sensitive relapsed ovarian cancer. N Engl J Med 366: 1382-1392, 2012.
5. Stańczyk M, Gromadzińska J and Wąsowicz W: Roles of reactive oxygen species and selected antioxidants in regulation of cellular metabolism. Int J Occup Med Environ Health 18: 15-26, 2005.
6. Okai Y, Sato EF, Higashi-Okai K and Inoue M: Potentiating effect of an endocrine disruptor, paranonylphenol, on the generation of reactive oxygen species (ROS) in human venous blood - association with the activation of signal transduction pathway. J UOEH 29: 221-233, 2007.
7. Moon HJ, Ko WK, Han SW, Kim DS, Hwang YS, Park HK and Kwon IK: Antioxidants, like coenzyme Q10, selenite, and curcumin, inhibited osteoclast differentiation by suppressing reactive oxygen species generation. Biochem Biophys Res Commun 418: 247-253, 2012.
8. Avni R, Cohen B and Neeman M: Hypoxic stress and cancer: imaging the axis of evil in tumor metastasis. NMR Biomed 24: 569-581, 2011.
9. Morita M, Yano S, Yamaguchi T, Yamauchi M and Sugimoto T: Phenylacetic acid stimulates reactive oxygen species generation and tumor necrosis factor-α secretion in vascular endothelial cells. Ther Apher Dial 15: 147-150, 2011.
10. Pak JH, Choi WH, Lee HM, et al: Peroxiredoxin 6 overexpression attenuates cisplatin-induced apoptosis in human ovarian cancer cells. Cancer Invest 29: 21- 28, 2011.
11. Lowther WT and Haynes AC: Reduction of cysteine sulfinic acid in eukaryotic, typical 2-Cys peroxiredoxins by sulfiredoxin. Antioxid Redox Signal 15: 99-109, 2011.
12. Aran M, Ferrero DS, Pagano E and Wolosiuk RA: Typical 2-Cys peroxiredoxins - modulation by covalent transformations and noncovalent interactions. FEBS J 276: 2478-2493, 2009.
13. Rhee SG and Woo HA: Multiple functions of peroxiredoxins: peroxidases, sensors and regulators of the intracellular messenger H_2O_2, and protein chaperones. Antioxid Redox Signal 15: 781-794, 2011.
14. Lin H, Lu JP, Laflamme P, et al: Inter-related in vitro effects of androgens, fatty acids and oxidative stress in prostate cancer: A mechanistic model supporting prevention strategies. Int J Oncol 37: 761-766, 2010.
15. Flohé L, Budde H and Hofmann B: Peroxiredoxins in antioxidant defense and redox regulation. Biofactors 19: 3-10, 2003.
16. Qiao B, Wang J, Xie J, Niu Y, Ye S, Wan Q and Ye Q: Detection and identification of peroxiredoxin 3 as a biomarker in hepatocellular carcinoma by a proteomic approach. Int J Mol Med 29: 832-840, 2012.
17. Kim YS, Lee HL, Lee KB, et al: Nuclear factor E2-related factor 2 dependent overexpression of sulfiredoxin and peroxiredoxin III in human lung cancer. Korean J Intern Med 26: 304-313, 2011.
18. Basu A, Banerjee H, Rojas H, et al: Differential expression of peroxiredoxins in prostate cancer: consistent upregulation of PRDX3 and PRDX4. Prostate 71: 755-765, 2011.
19. Dai Z, Yin J, He H, et al: Mitochondrial comparative proteomics of human ovarian cancer cells and their platinum-resistant sublines. Proteomics 10: 3789-3799, 2010.
20. Lee S, Kwon H, Jeong K and Pak Y: Regulation of cancer cell proliferation by caveolin-2 down-regulation and re-expression. Int J Oncol 38: 1395-1402, 2011.
21. Jemal A, Siegel R, Ward E, Hao Y, Xu J, Murray T and Thun MJ: Cancer statistics, 2008. CA Cancer J Clin 58: 71-96, 2008.
22. Bookman MA: Developmental chemotherapy and management of recurrent ovarian cancer. J Clin Oncol 21 (10 Suppl): 149s-167s, 2003.
23. Young TW, Mei FC, Yang G, Thompson-Lanza JA, Liu J and Cheng X: Activation of antioxidant pathways in ras-mediated oncogenic transformation of human surface ovarian epithelial cells revealed by functional proteomics and mass spectrometry. Cancer Res 64: 4577-4584, 2004.
24. Oiso S, Ikeda R, Nakamura K, Takeda Y, Akiyama S and Kariyazono H: Involvement of NF-κB activation in the cisplatin resistance of human epidermoid carcinoma KCP-4 cells. Oncol Rep 28: 27-32, 2012.
25. Sethi G, Sung B and Aggarwal BB: Nuclear factor-kappaB activation: from bench to bedside. Exp Biol Med (Maywood) 233: 21-31, 2008.